

Electronic Supplementary Information

Scalable and controllable fabrication of CNTs improved yolk-shelled Si anode with advanced in-operando mechanical quantification

Lei Zhang^{a,b‡}, Qianwei Huang^{c‡}, Xiaozhou Liao^c, Yuhai Dou^a, Porun Liu^a, Mohammad Al-Mamun^a, Yun Wang^a, Shanqing Zhang^a, Shenlong Zhao^c, Dan Wang,^{a,d} Guowen Meng^{b*}, Huijun Zhao^{a*}*

^a Centre for Clean Environment and Energy, Gold Coast Campus, Griffith University, Gold Coast, QLD 4222, Australia

^b Key Laboratory of Materials Physics, and Anhui Key Laboratory of Nanomaterials and Nanotechnology, CAS Center for Excellence in Nanoscience, Institute of Solid State Physics, Chinese Academy of Sciences, P. O. Box 1129, Hefei 230031, China

^c School of Aerospace, Mechanical and Mechatronics Engineering, The University of Sydney, Sydney, NSW, 2006, Australia

^d State Key Laboratory of Biochemical Engineering, CAS Center for Excellence in Nanoscience, Institute of Process Engineering, Chinese Academy of Sciences, No. 1 Beiertiao, Zhongguancun, Beijing 100190, P. R. China

Lei Zhang and Qianwei Huang: These authors contributed equally to this work.

Correspondence and requests for materials should be addressed to H.Z. (email: h.zhao@griffith.edu.au) D.W. (danwang@ipe.ac.cn), and G.W.M. (gwmeng@issp.ac.cn)

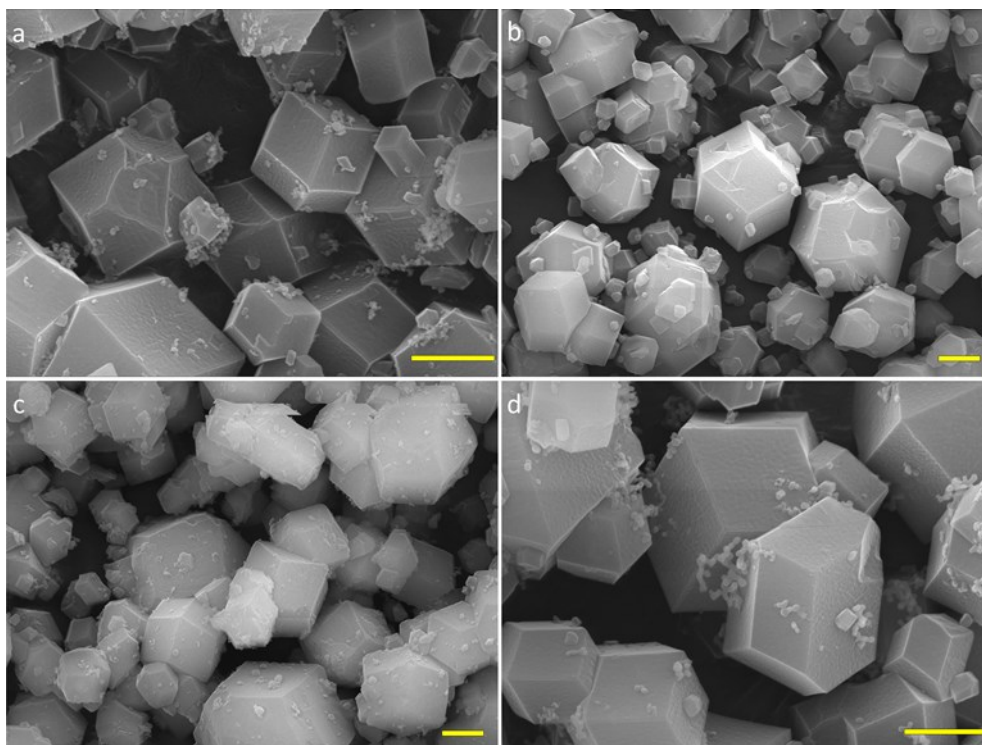


Fig. S1. SEM images of ZIF-Si. **a**, ZIF-8-Si. **b**, ZIF-67/ZIF-8-Si. **c**, ZIF-8/ZIF-67-Si. **d**, ZIF-67-Si. Scale bar: 1 μm . All of the ZIF-Si samples are dodecahedron-shaped microcrystals with sizes ranged from 1.0 to 5.0 μm .

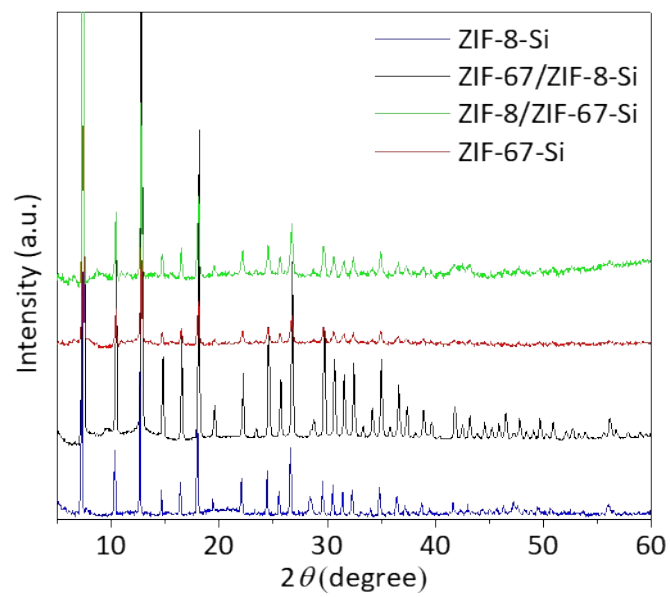


Fig. S2. XRD patterns of ZIF-Si samples. All observed peaks from the ZIF-Si samples can be assigned to ZIF-67, ZIF-8 and Si.

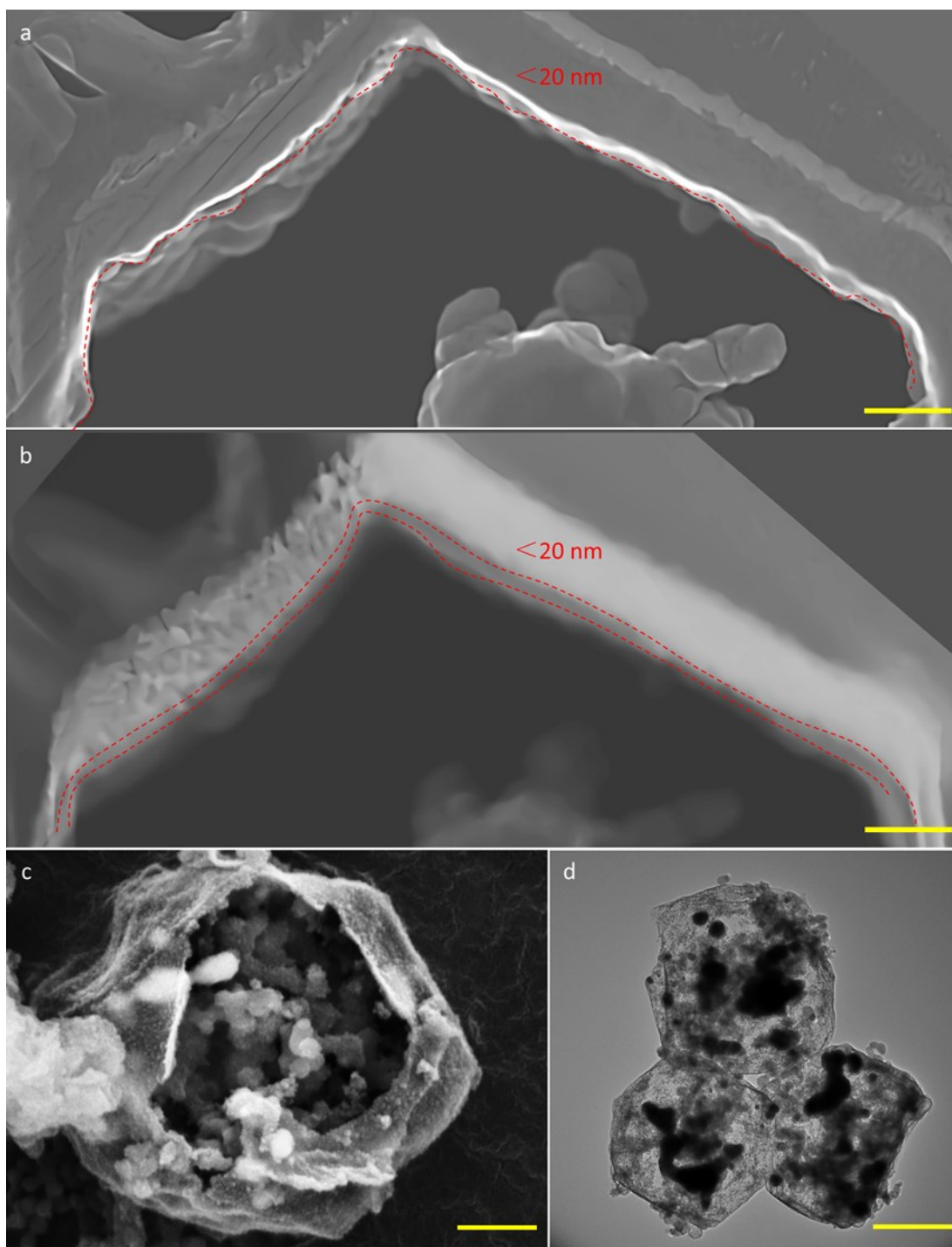


Fig. S3. Morphological and structural characteristics of Si/C. **(a, b)**, Cross-sectional SEM and TEM images of Si/C shell (Scale bar: 100 nm). **c**, SEM image of a broken Si/C unit (Scale bar: 500 nm). **d**, Low magnification TEM image of Si/C (Scale bar: 500 nm).

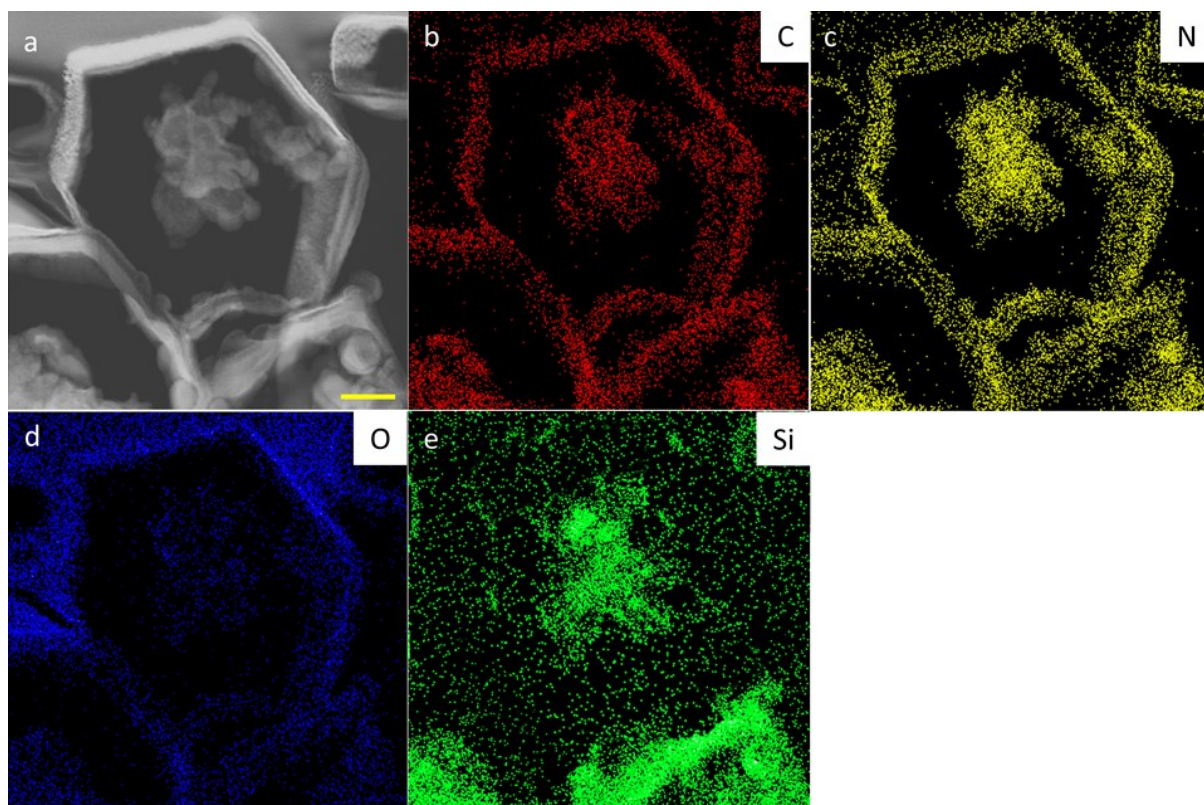


Fig. S4. **a**, TEM image of Si/C. **(b-e)**, EDS mapping images of Si/C. Scale bar: 200 nm.

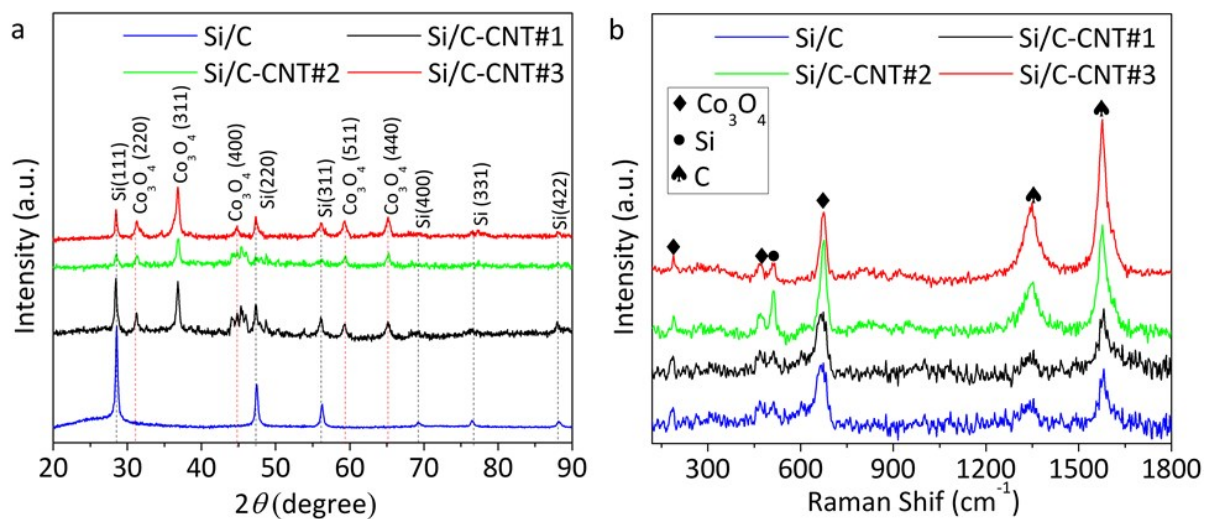


Fig. S5. a, XRD patterns of Si/C and Si/C-CNT samples. **b**, Raman spectra of Si/C and Si/C-CNT samples.

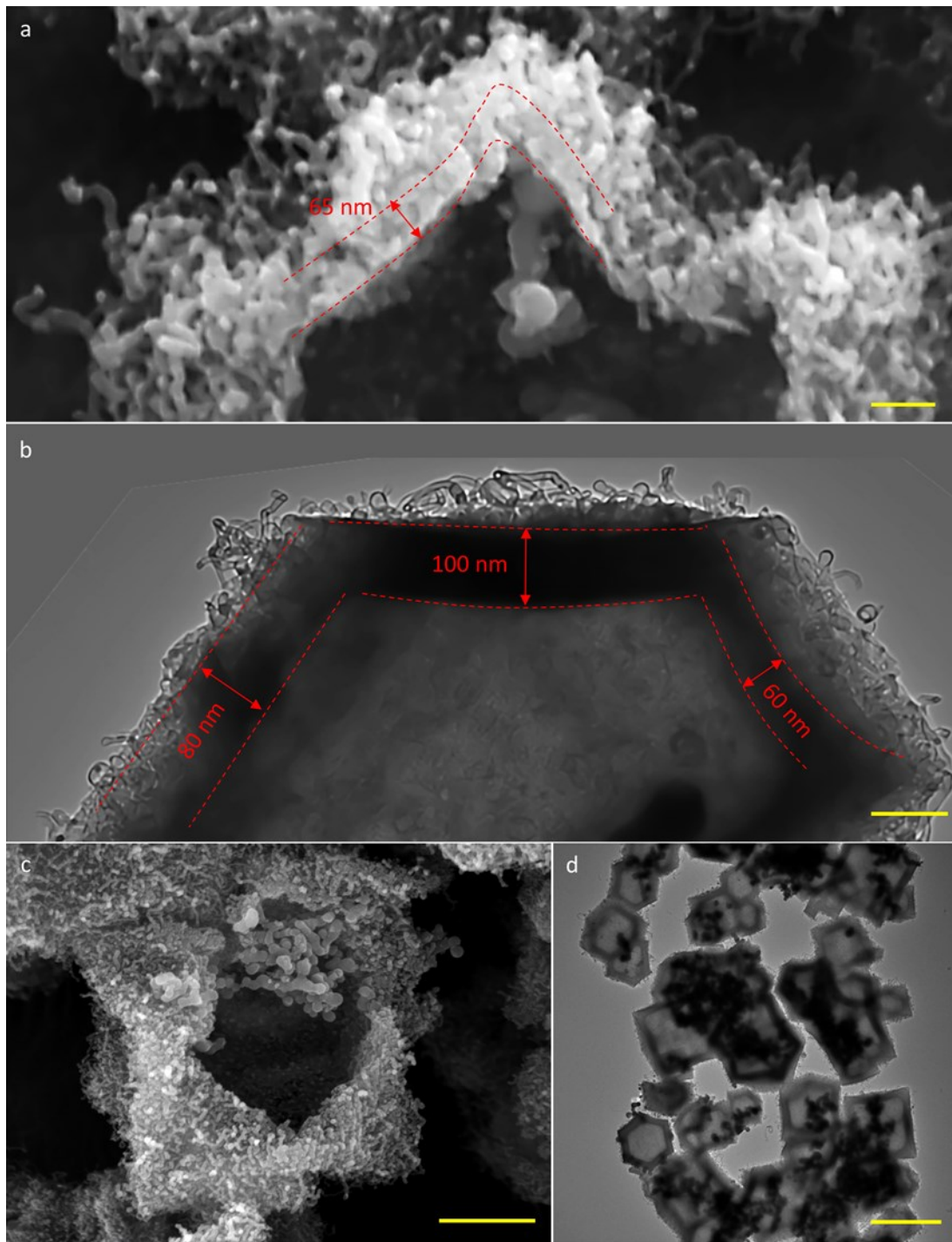


Fig. S6. Morphological and structural characteristics of Si/C-CNT#1. **(a, b)**, Cross-sectional SEM and TEM images of Si/C-CNT#1 shell (Scale bar: 100 nm). **c**, SEM image of a broken Si/C-CNT#1 unit (Scale bar: 500 nm). **d**, Low magnification TEM image of Si/C-CNT-1 (Scale bar: 500 nm).

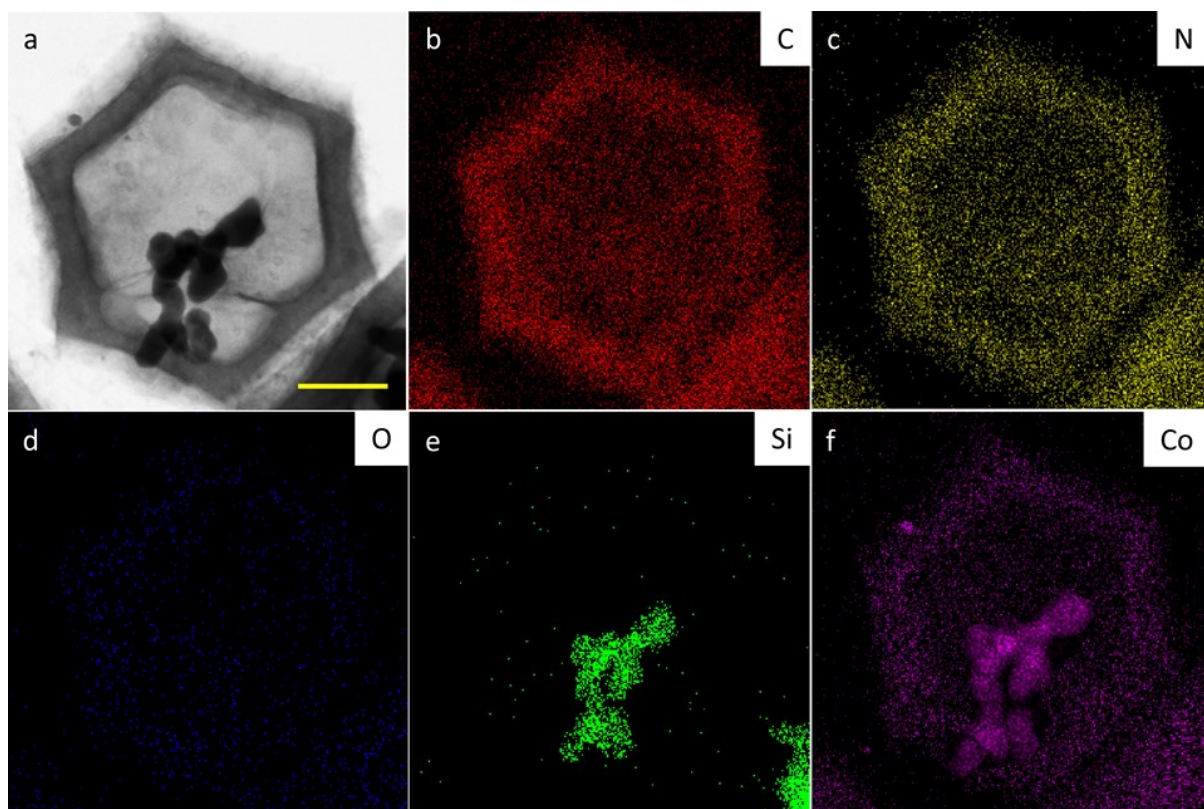


Fig. S7. a, TEM and **(b-f)**, EDS mapping images of Si/C-CNT#1. Scale bar: 200 nm.

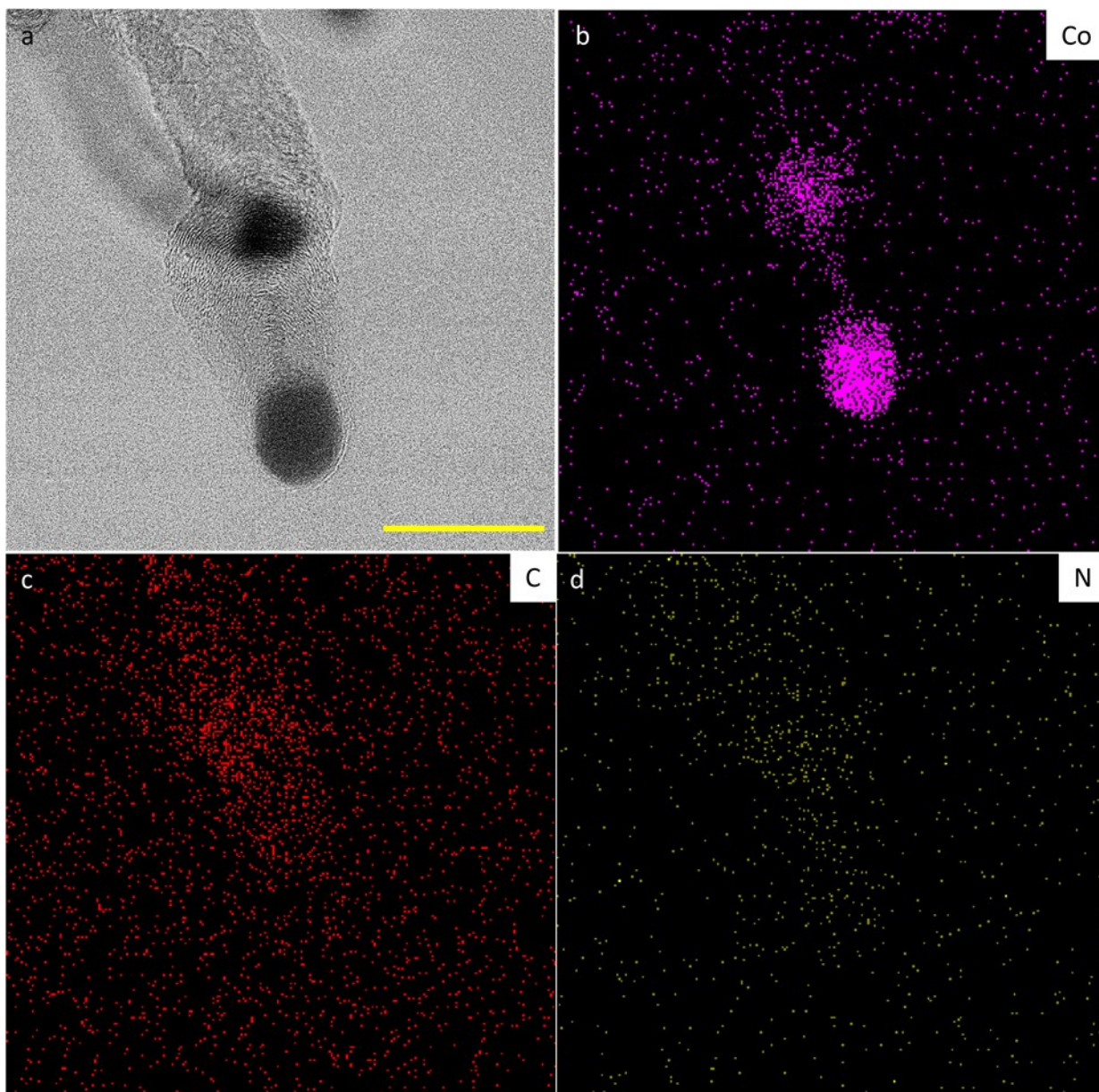


Fig. S8. a, HRTEM and (b-d), EDS mapping images of CNTs-Co₃O₄ NPs on the outer surface of Si/C-CNT#1. Scale bar: 20 nm.

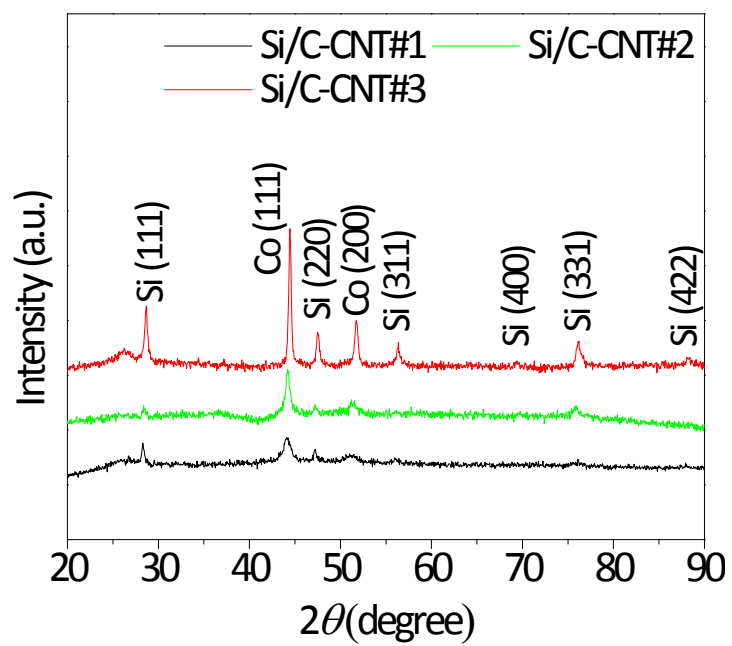


Fig. S9. XRD patterns of Si/C-CNT samples before air oxidation treatment.

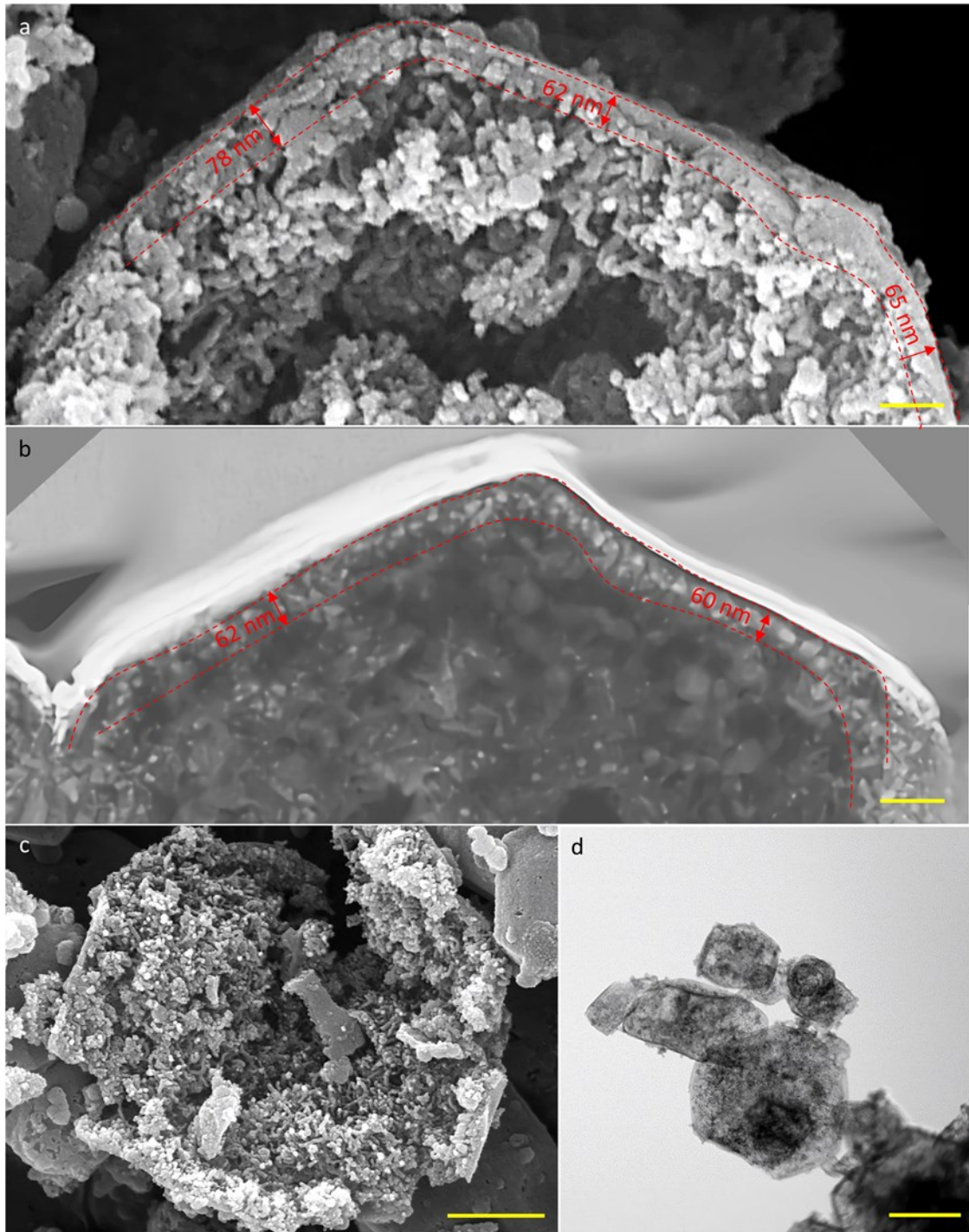


Fig. S10. Morphological and structural characteristics of Si/C-CNT#2. **(a, b)**, Cross-sectional SEM and TEM images of Si/C-CNT#2 shell (Scale bar: 100 nm). **c**, SEM image of a broken Si/C-CNT#2 unit (Scale bar: 500 nm). **d**, Low magnification TEM image of Si/C-CNT-2 (Scale bar: 1 μm).

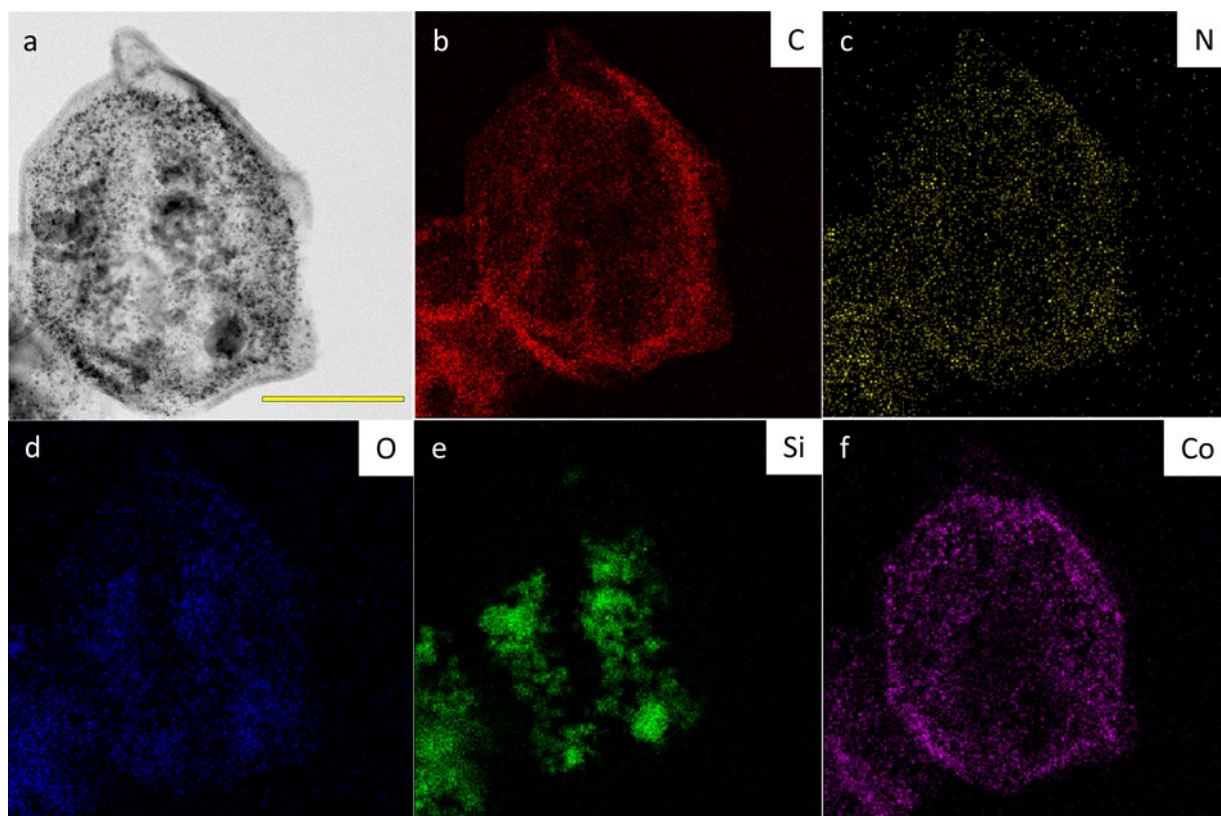


Fig. S11. a, TEM and **(b-f),** EDS mapping images of Si/C-CNT#2. Scale bar: 500 nm.

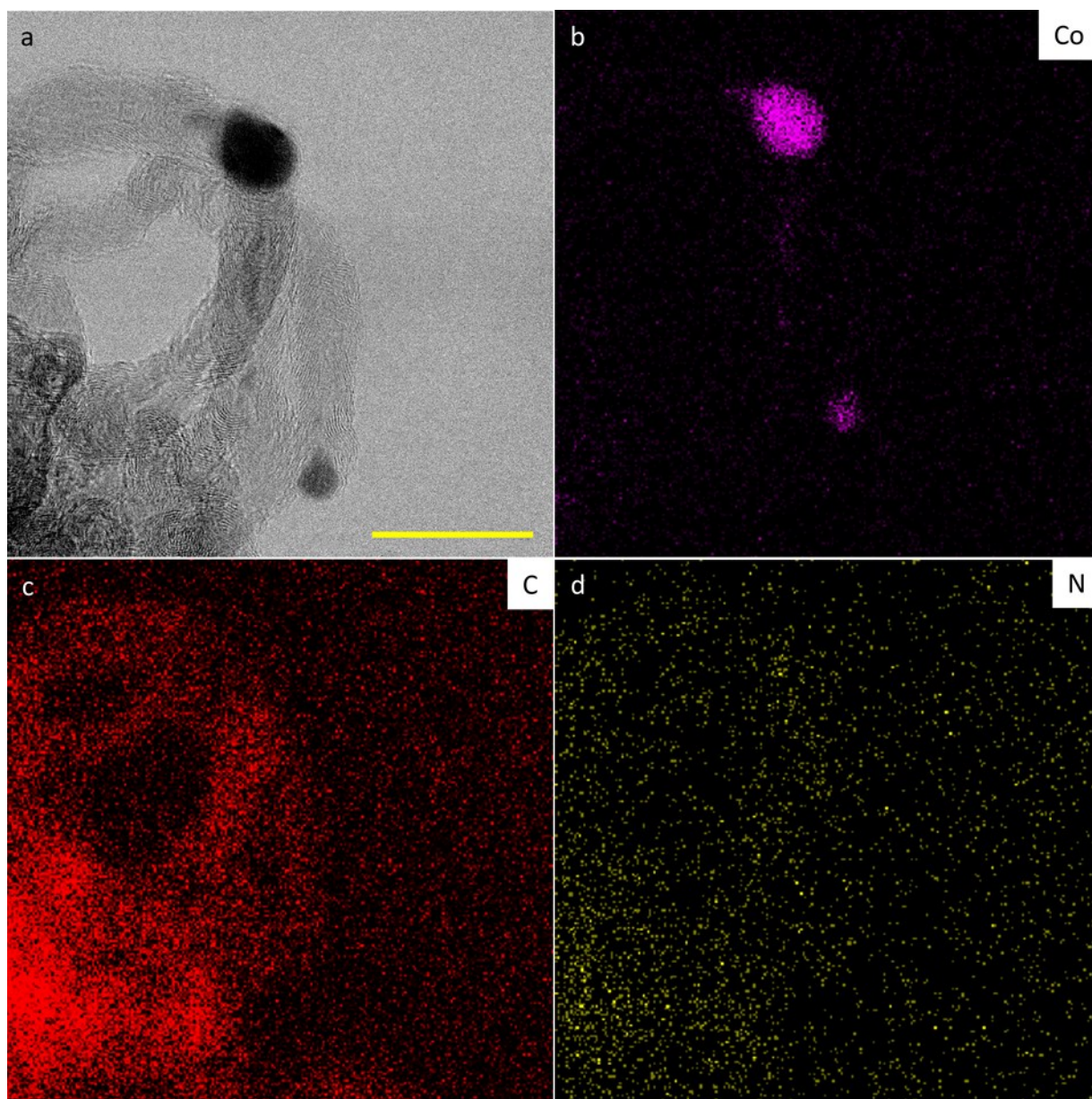


Fig. S12. a, HRTEM and (b-d), EDS mapping images of CNTs- Co_3O_4 NPs on the inner surface of Si/C-CNT#2. Scale bar: 20 nm.

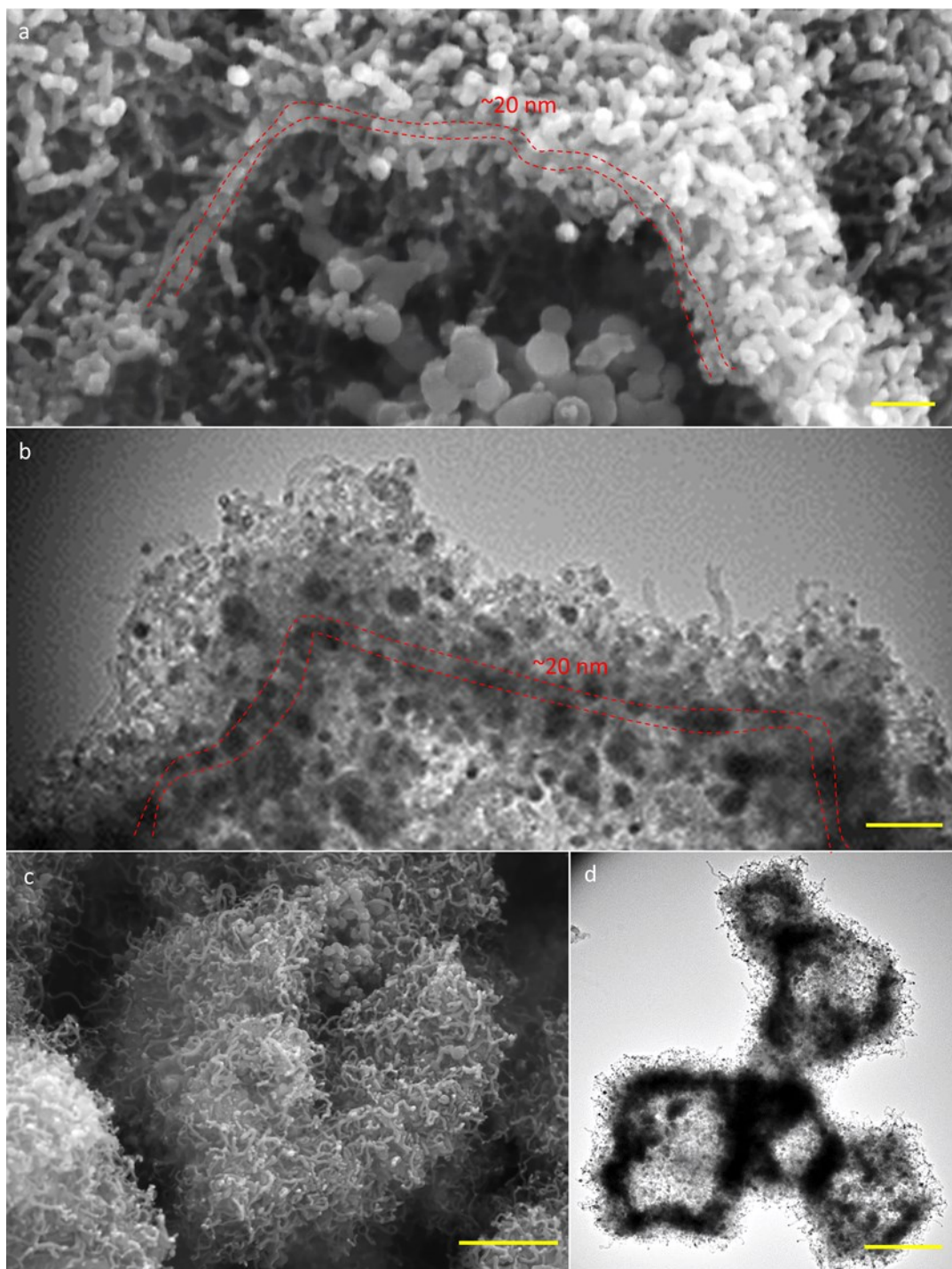


Fig. S13. Morphological and structural characteristics of Si/C-CNT#3. (a, b), Cross-sectional SEM and TEM images of Si/C-CNT#3 shell (Scale bar: 100 nm). c, SEM image of a broken Si/C-CNT#3 unit (Scale bar: 500 nm). d, Low magnification TEM image of Si/C-CNT-3 (Scale bar: 1 μm).

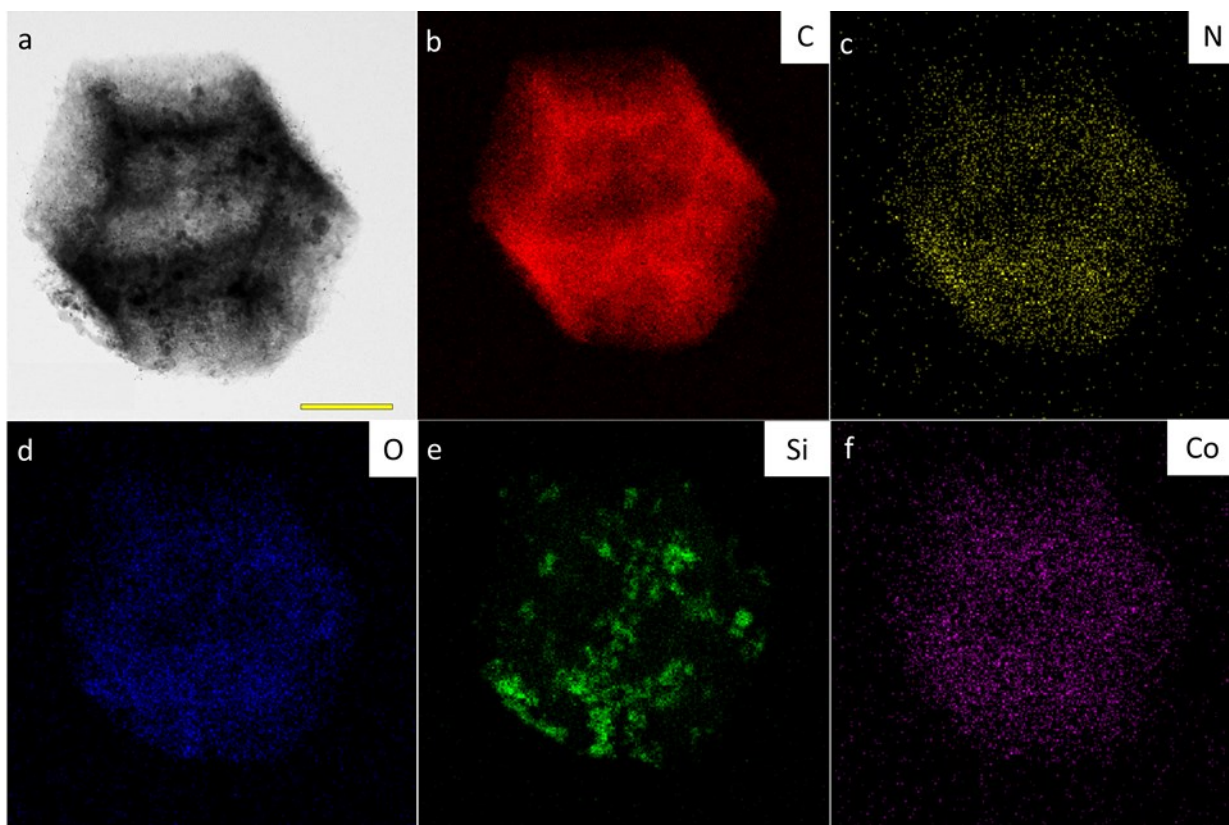


Fig. S14. a, TEM and (b-f), EDS mapping images of Si/C-CNT#3. Scale bar: 500 nm.

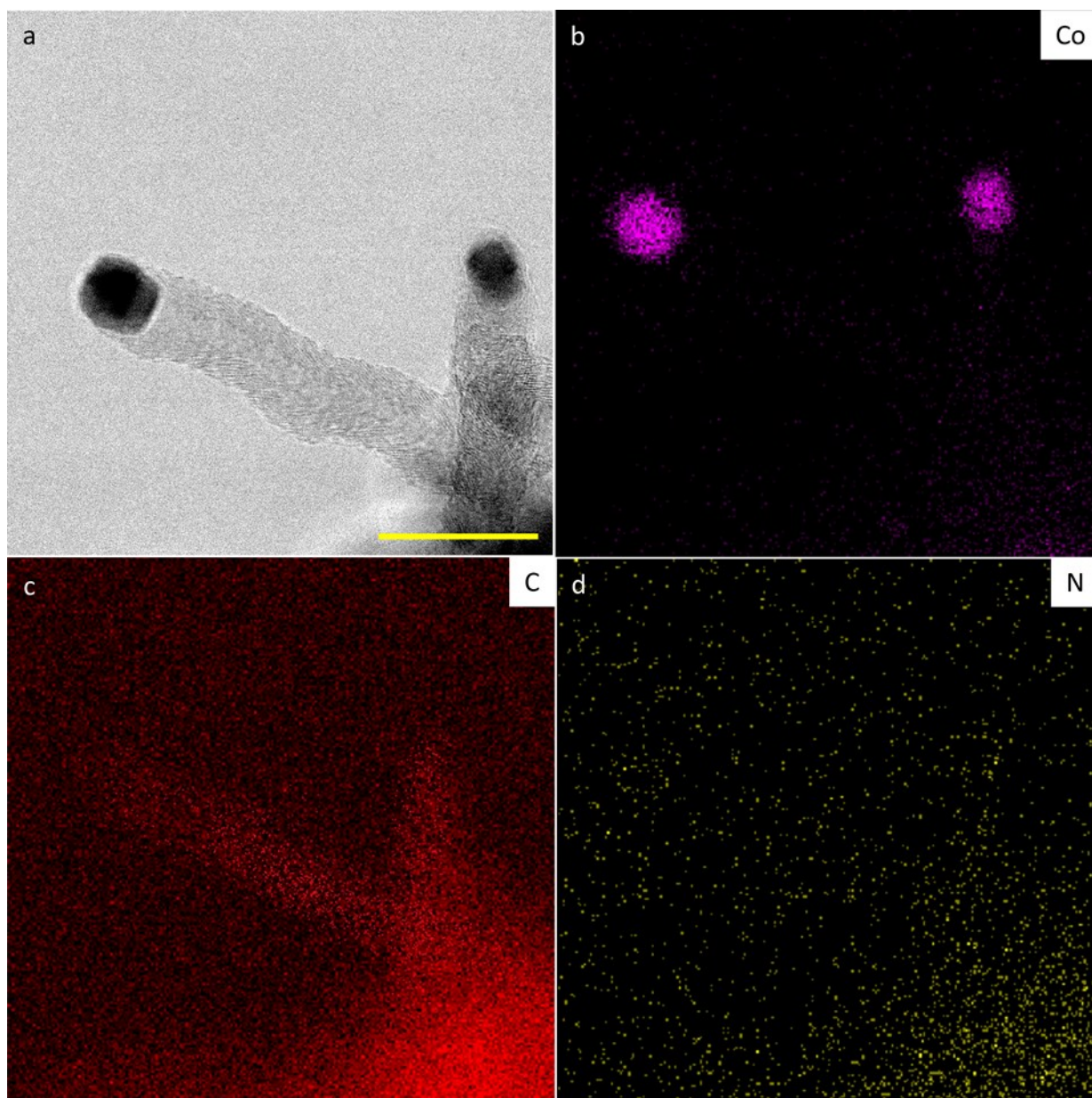


Fig. S15. a, HRTEM and **(b-d),** EDS mapping images of CNTs- Co_3O_4 NPs on the outer surface of Si/C-CNT#3. Scale bar: 20 nm.

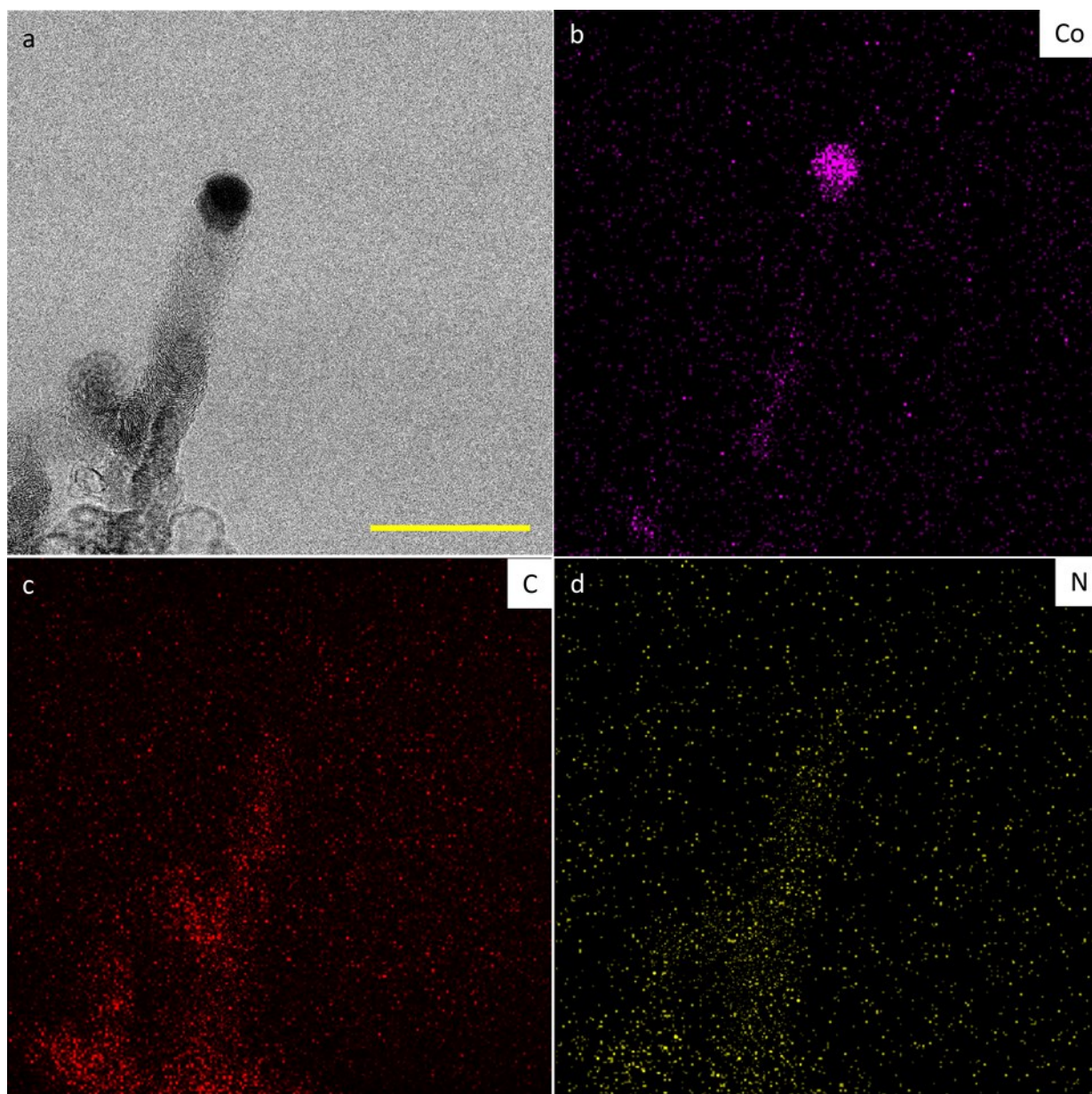


Fig. S16. HRTEM and (b-d), EDS mapping images of CNTs-Co₃O₄ NPs on the inner surface of Si/C-CNT#3. Scale bar: 20 nm.

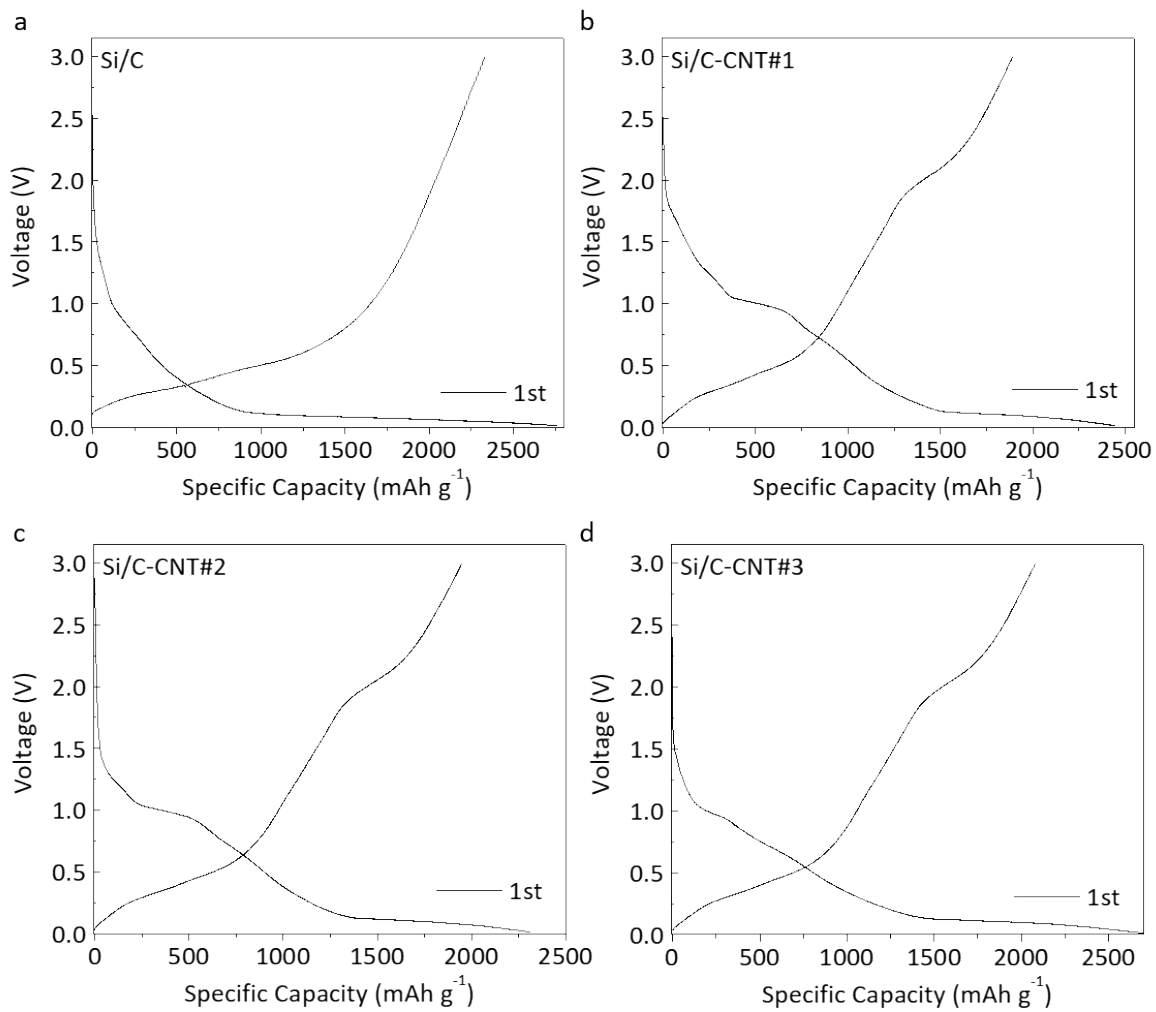


Fig. S17. Initial discharge-charge profiles of **a**, Si/C, **b**, Si/C-CNT#1, **c**, Si/C-CNT#2 and **d**, Si/C-CNT#3. Voltage range: 0.01 V–3.0 V. Current density: 0.1 A g^{-1} .

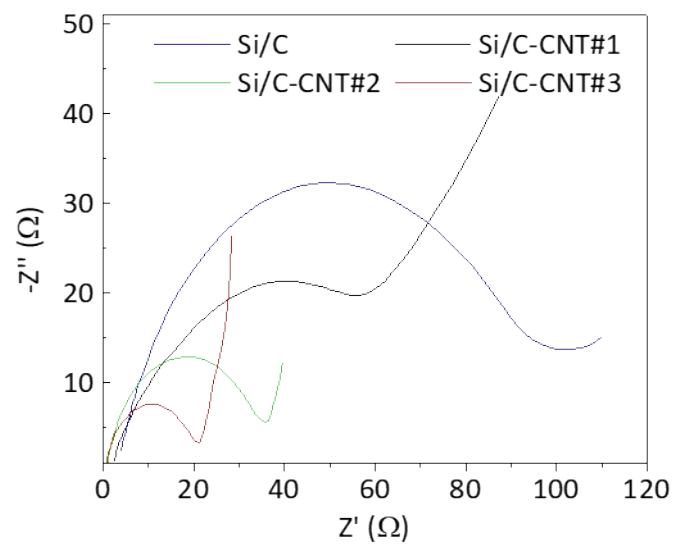


Fig. S18. Nyquist plots of Si/C and Si/C-CNT samples.

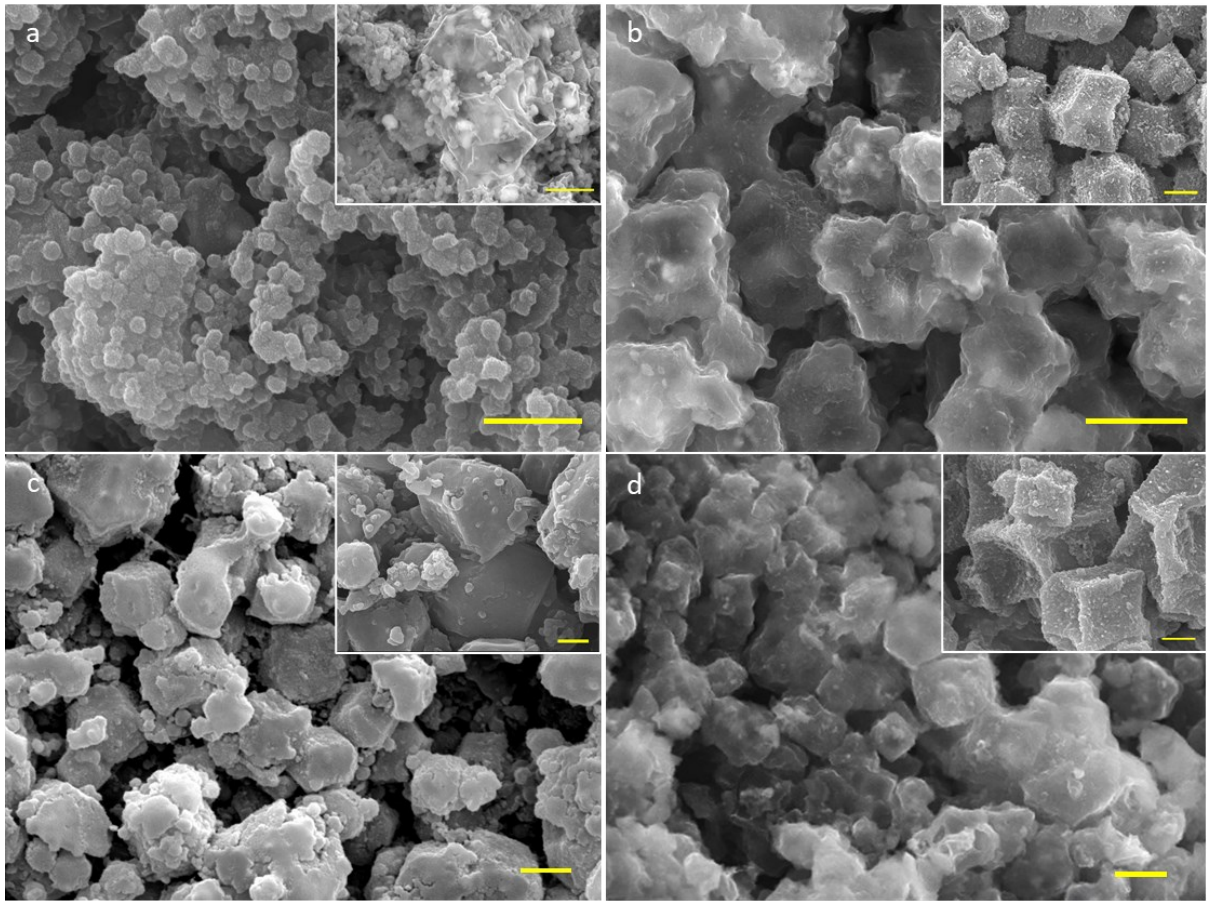


Fig. S19. SEM images of **a**, Si/C, **b**, Si/C-CNT#1, **c**, Si/C-CNT#2 and **d**, Si/C-CNT#3 after cycling test. Scale bar: 1 μm . Inserts are the SEM image of samples before cycling test. Scale bar: 500 nm.

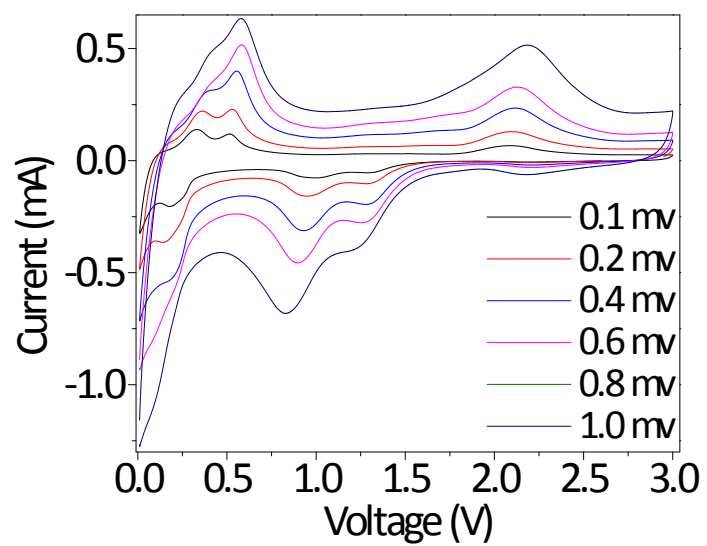


Fig. S20. CVs of Si/C-CNT#3 at different scan rates from 0.1 to 1.0 mV s⁻¹ within a voltage range of 0.01–3.0 V.

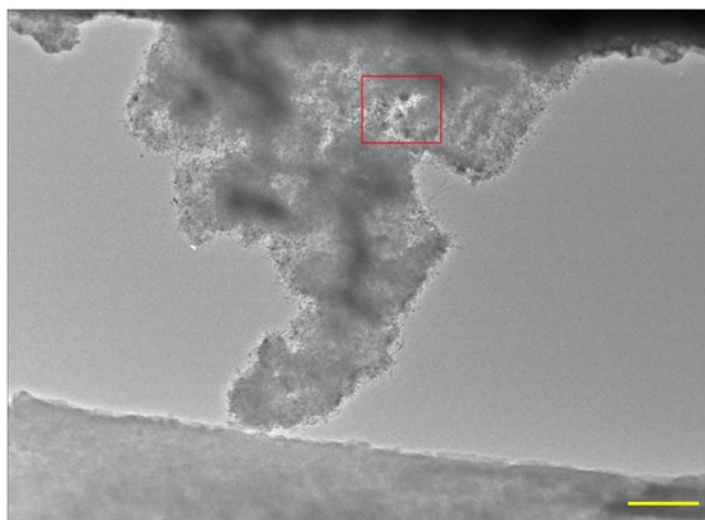


Fig. S21. In-operando recorded TEM image for a cluster of Si/C-CNT#3 units immobilised on the copper grid-working electrode. Red line enclosed area indicates the targeted set of Si NPs inside a Si/C-CNT#3 unit. Scale bar: 500 nm.

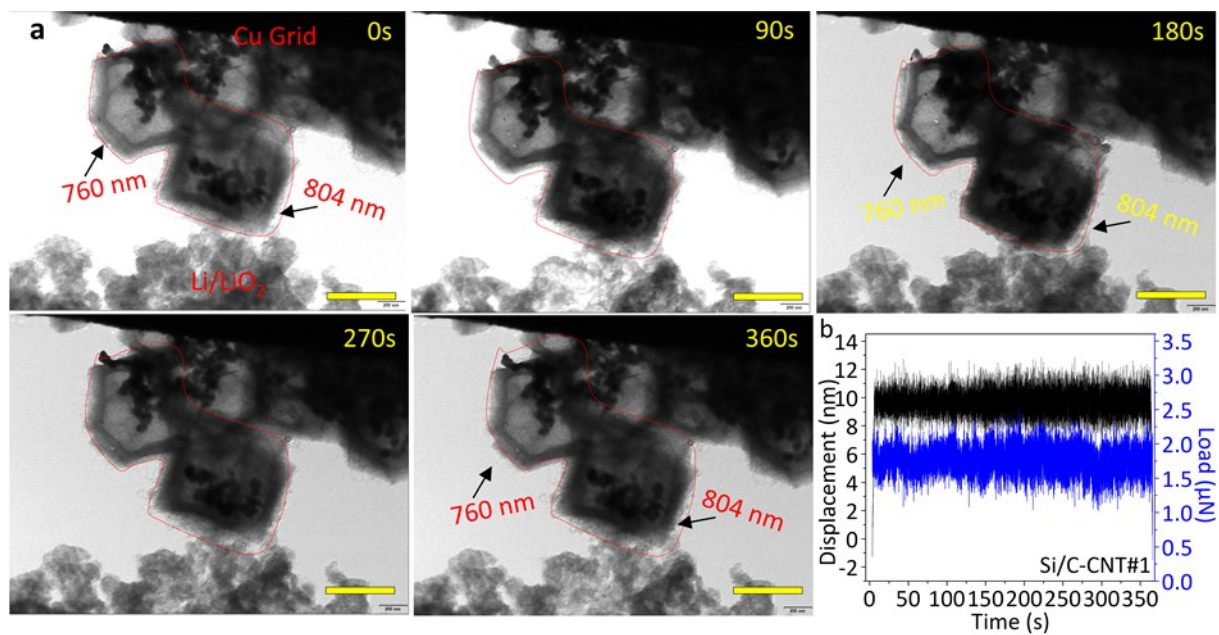


Fig. S22. **a**, Time-lapsed in-operando TEM images of the targeted cluster of Si/C-CNT#1 units during lithiation (0-180 s)/delithiation (180-360 s). **b**, Load- and displacement-time profiles during lithiation/delithiation. Scale bar: 500 nm.

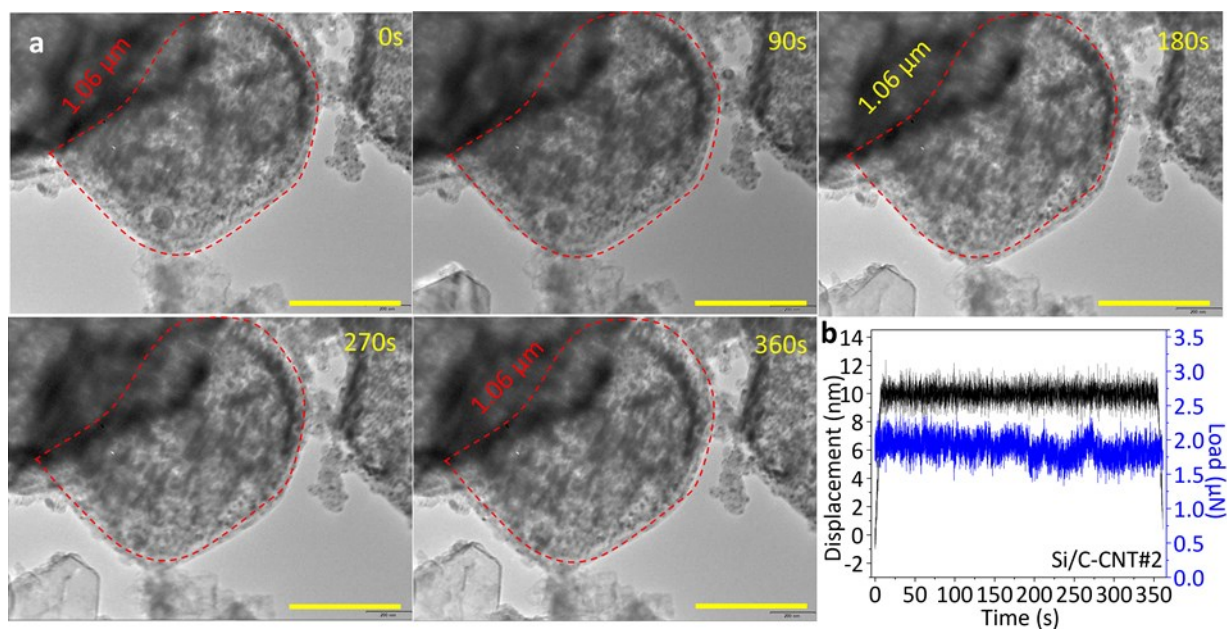


Fig. S23. a, Time-lapsed in-operando TEM images of the targeted cluster of Si/C-CNT#2 units during lithiation (0-180 s)/delithiation (180-360 s). **b**, Load- and displacement-time profiles during lithiation/delithiation. Scale bar: 500 nm.

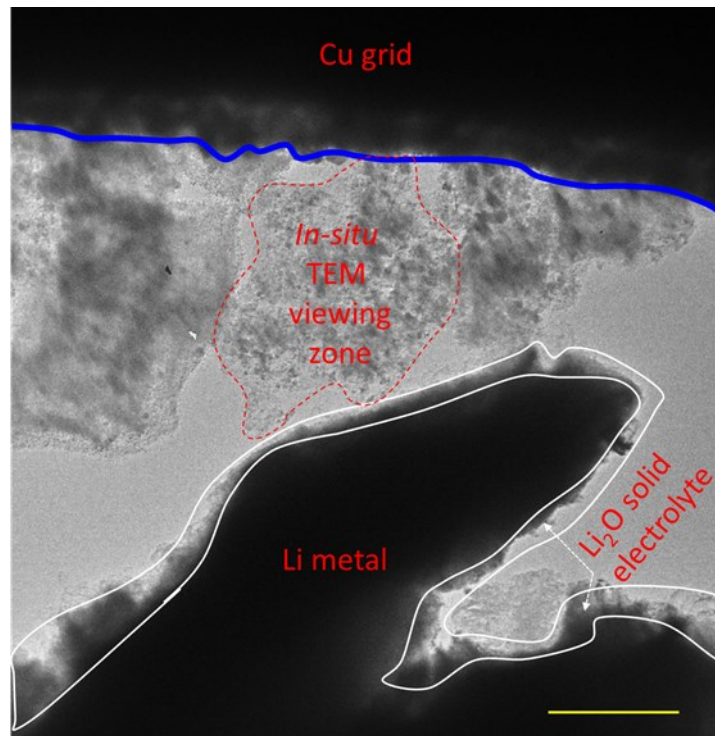


Fig. S24. Assembled TEM electrochemical measurement cell before inducing Li dendrite. Red line enclosed area shows the *in-situ* TEM viewing zone on a Si/C-CNT#3 structure unit. Scale bar: 1 μm .

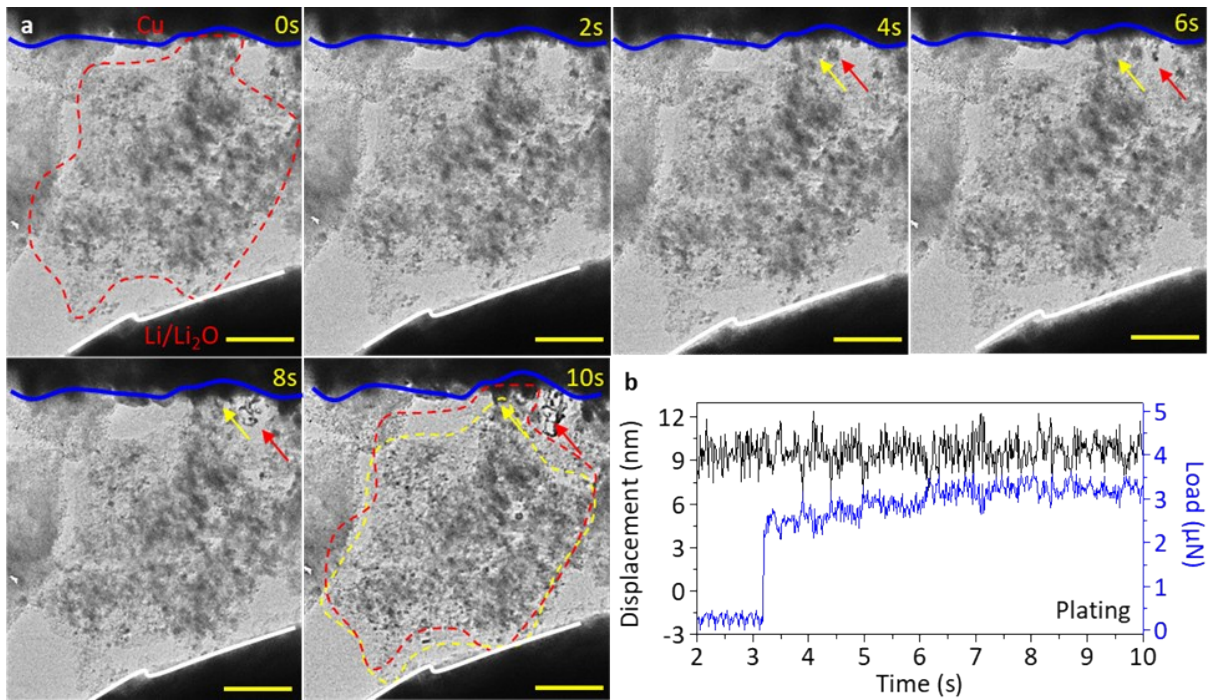


Fig. S25. **a**, Time-lapsed in-operando TEM images of Si/C-CNT#3 during the first 10 s of Li plating process. Scale bar: 500 nm. **b**, Corresponding load- and displacement-time profiles.

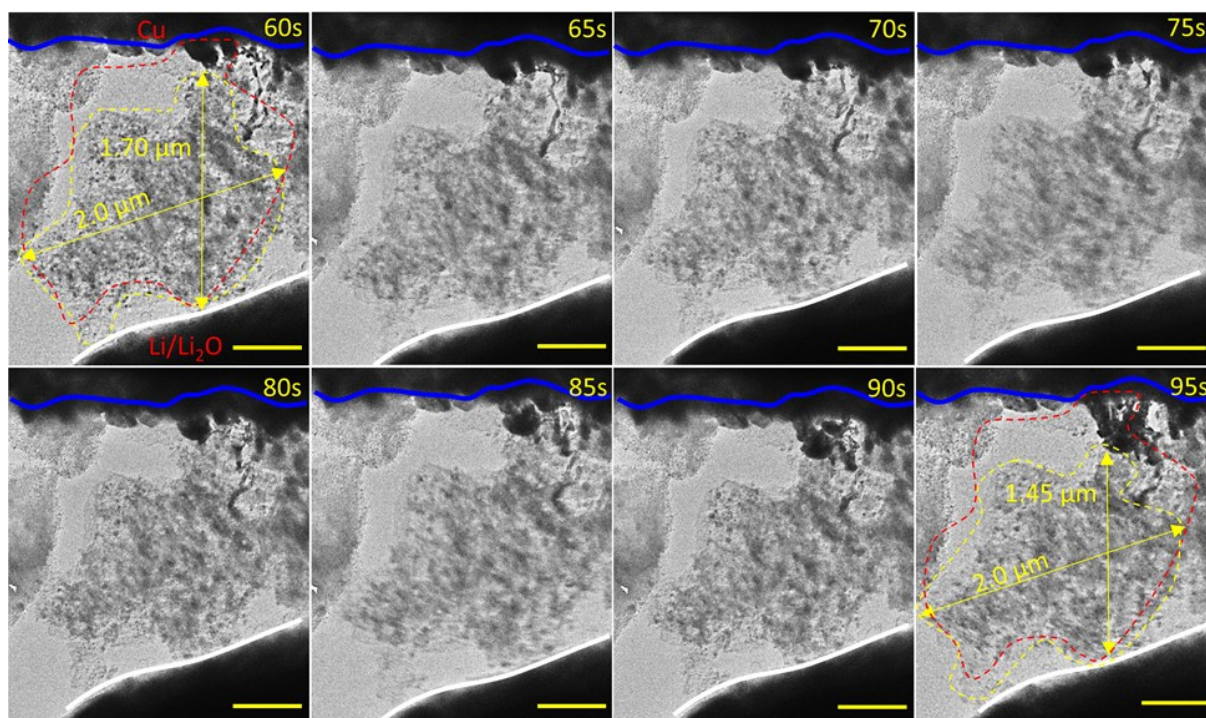


Fig. S26. Time-lapsed in-operando TEM images of the Si/C-CNT#3 during Li plating process between 60 and 95 s. Scale bar: 500 nm.

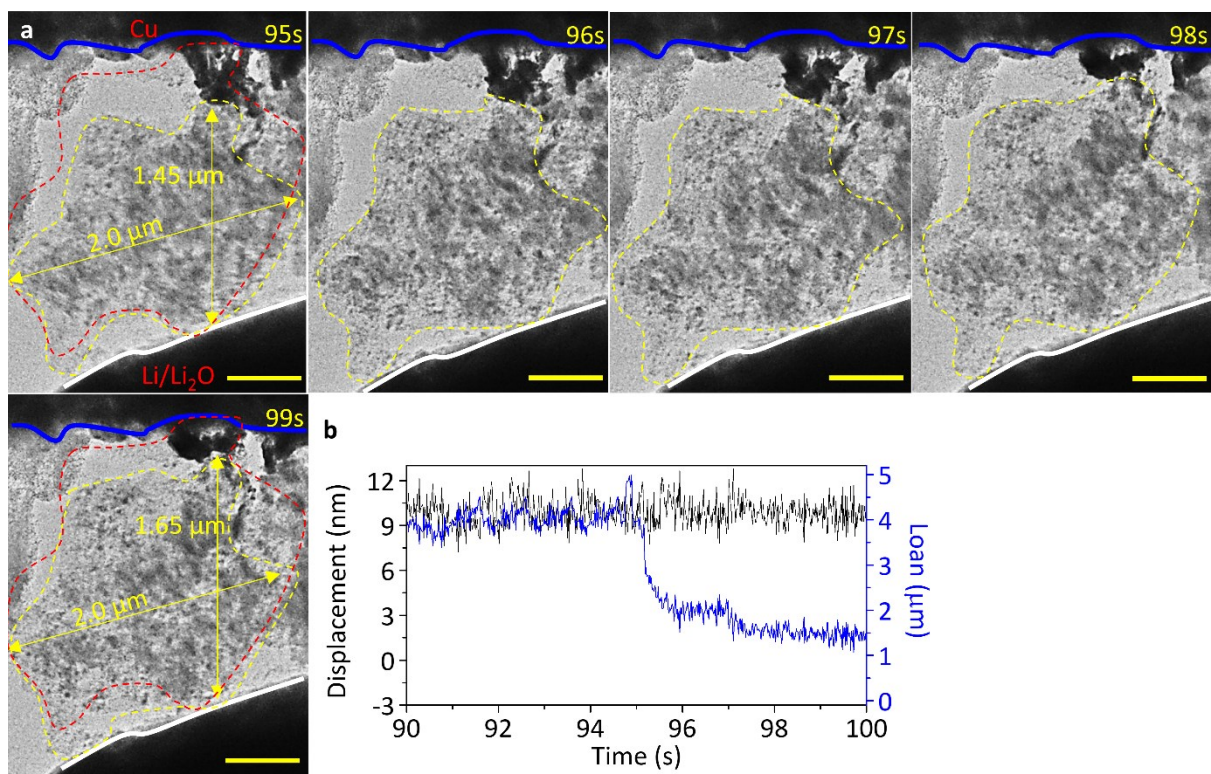


Fig. S27. **a**, Time-lapsed in-operando TEM images of the Si/C-CNT#3 during Li plating process between 95 and 99 s. Scale bar: 500 nm. **b**, Corresponding load- and displacement-time profiles.

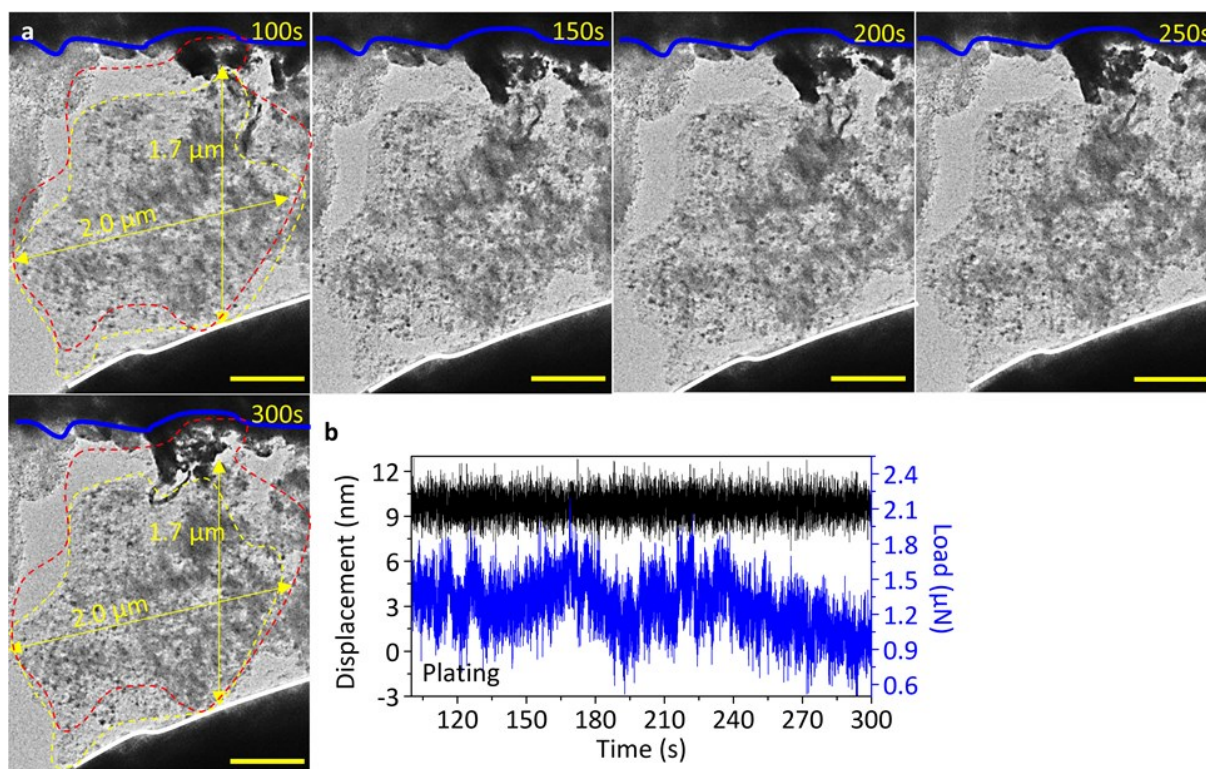


Fig. S28. **a**, Time-lapsed in-operando TEM images of the Si/C-CNT#3 during Li plating process between 100 and 300 s. Scale bar: 500 nm. **b**, Corresponding load- and displacement-time profiles.

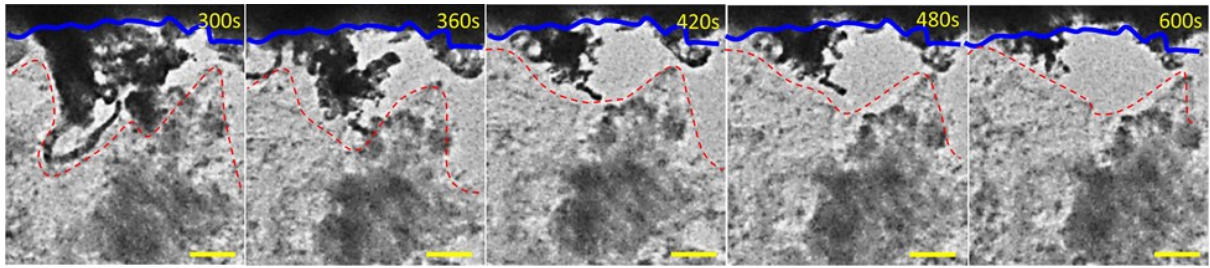


Fig. S29. Time-lapsed in-operando high magnification TEM images showing Li dendrites dissolution process. Scale bar: 100 nm.